Robust Reconfigurable Control for In-Wheel Electric Vehicles

Péter Gáspár

Institute of Computer Science and Automation
MTA-BME Control Engineering Research Group
Hungarian Academy of Sciences
H-1111 Budapest, Kende u 13-17, HUNGARY

Abstract – *The paper presents the control design of a vehicle, which is driven by four independently driven in-wheel electric motors and steered by the steering system. The direction of the vehicle is based on the steering, while driving and braking are based on the electric motors. Since the direction can also be modified by the appropriate operation of the four electric motors, reconfigurable and fault-tolerant control systems can be designed. When a vehicle skids, or a failure occurs in one of the electric motors or in the steering, the reconfigurable control is activated. The reconfigurable control is realized based on robust LPV control design methods, in which performance degradations and fault scenarios are also built. The operation of the designed control system is demonstrated in a CarSim simulation environment.*

Keywords: LPV control, trajectory tracking, vehicle control.

1 Introduction

Owing to the growing demand for environmentally friendly and economical transportation, in-wheel electric vehicles receive increasing attention from automotive companies and researchers as well. These vehicles with hub motors integrated in two or four wheels have several advantages and very few drawbacks compared to conventional vehicles with internal combustion engines. The compact size of in-wheel motors and the absence of regular drive train components (gearbox, differential, etc.) enable space-efficient passenger cabin design, also resulting in reduced overall weight. However, the increased unsprung mass of the vehicle may lead to adverse vertical vibrations, which may affect the ride comfort and stability of the in-wheel electric vehicle especially in fast motions over bumps. From a vehicle control point of view the most appealing properties of the independently-controllable in-wheel motors are the fast and accurate torque generation, enabling the design of very effective stabilizing and anti-slip systems.

Recent studies of in-wheel vehicles focus on exploiting the specific properties of the electric hub motors. High-performance wheel-slip control was proposed by several authors, see [2],[7]. Lateral control of in-wheel vehicles was also proposed by [9],[10],[13]. Rollover avoidance methods were proposed by [6]. The performance of in-wheel motors may degrade due to mechanical failures, the overheating of the engine or faults connected to the motor control system. A fault-tolerant control system designed to accommodate hub motor faults by automatically reallocating the control effort among other healthy wheels was proposed by [4],[5],[11]. The control system is also able to handle the effects of the failure or performance degradation of the steering system, with the appropriate acceleration/brake of the four electric motors, the direction of the vehicle can be modified.

In the paper the control design of a vehicle which is driven by four independently driven in-wheel electric motors and steered by the steering system is proposed. The control is augmented with reconfigurable and fault-tolerant features in order to handle various cases such as the skidding of a wheel, a failure of one of the electric motors or a failure of the steering. The control reconfiguration method is used to avoid emergencies resulting from adhesion loss or fault events. The realization of the yaw moment demanded by the high-level control is controlled by a supervisor, and the appropriate correction moment can be created. In the low-level control in-wheel motor torques are generated by the physical actuators. The main novelty of the paper lies in the high-level LPV control design and the reconfiguration method in the low level applied for performance degradation and fault cases. The goal of the design is to perform the predefined velocity and road trajectory of the vehicle even when performance degradation or a fault occurs in the system.

The paper is organized as follows: Section 2 presents the control problem and the control-oriented dynamic model. Section 3 focuses on the robust and reconfigurable trajectory tracking controller based on the LPV framework and the allocation of the control signals. Section 4 shows the operation of the control system in a high-fidelity simulation environment. Finally, some concluding remarks are presented in Section 5.

2 Vehicle model for trajectory tracking

The purpose of the control design is to guarantee both velocity and road trajectory tracking for the in-wheel electric vehicle. In the design both the longitudinal and the lateral dynamics of the vehicle are considered, while the vertical motion is ignored. The motion equation of the vehicle is based on the reduced nonlinear two-track bicycle model, see Figure 1.

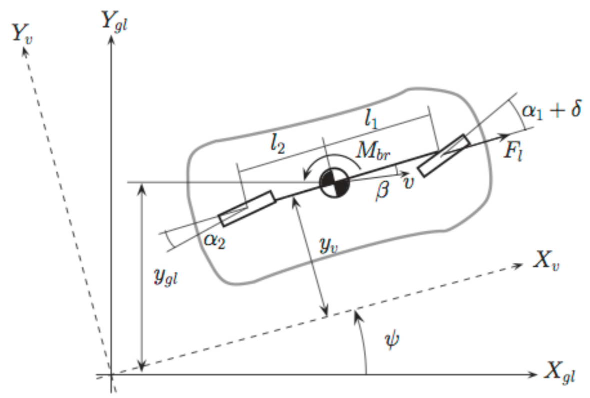

Figure 1: Single track bicycle model

The model for trajectory tracking in the plane is formed by the yaw, the lateral and the longitudinal dynamics. The vehicle yaw angle, the side-slip angle and the longitudinal displacement are denoted by ψ, β, ξ, respectively. The motion equations of the model are as follows:

$$J\ddot{\psi} = c_1 l_1 \alpha_f - c_2 l_2 \alpha_r + M_z \quad (1)$$
$$m\dot{\xi}(\dot{\psi} + \dot{\beta}) = c_1 \alpha_f + c_2 \alpha_r \quad (2)$$
$$m\ddot{\xi} = F_l - F_d \quad (3)$$

where m is the total mass, J is yaw inertia, l_1 and l_2 are geometric parameters related to the front and rear axle positions, c_1 and c_2 are cornering stiffnesses of the tires and $\alpha_f = \delta - \beta - \dot{\psi} l_1/\dot{\xi}$, $\alpha_r = -\beta + \dot{\psi} l_2/\dot{\xi}$ are the side-slip angle at the front and the rear. Note that system nonlinearity is caused by longitudinal velocity $\dot{\xi}$.

The control inputs of the system are the longitudinal force F_l and the yaw moment M_z generated by the in-wheel motors, and, moreover, the front steering angle δ generated by the steering system.

The disturbance force F_d consists of three elements, which are the following: disturbance due to the road slope $F_{d1} = mgsin\alpha$, where α is the angle of the road slope; drag disturbance given by $F_{d2} = c_w \rho A \dot{\xi}^2/2$, where c_w is the drag co-efficient, ρ is air mass density, A is the frontal area contact surface of the vehicle; the rolling resistance given by $F_{d3} = mgK\cos\alpha$ where K is the road surface.

The differential equations of the trajectory tracking are converted into a state-space form:

$$\dot{x} = A(\rho_1)x + B_1 w + B_2(\rho_2)u \quad (4)$$

where the state vector of the system is $x = [\dot{\xi} \quad \xi \quad \dot{\psi} \quad \beta]^T$, the vector of the control inputs is $u = [F_l \quad \delta \quad M_z]^T$, the measured outputs are the velocity and the yaw rate, i.e., $y = [\dot{\xi} \quad \dot{\psi}]^T$ and the disturbance is represented by the disturbance force $w = [F_d]^T$.

Since velocity and the road trajectory tracking of the vehicle are required, it is necessary to define the reference signals. For the control both the reference velocity and the reference yaw rate are given as predefined signals. The vehicle model described by (1)…(3) is nonlinear with the quadratic parameter $\dot{\xi}$, thus for a general solution a gain scheduling LPV controller must be designed. For the longitudinal control the desired velocity $\dot{\xi}_{ref}$ is predefined.

Yaw-rate control design has been studied by a number of authors, see e.g. [8]. For the lateral control of the vehicle the reference yaw-rate is predefined by the road curvature as follows:

$$\dot{\psi}_{ref} = \frac{\dot{\xi}}{r} \quad (5)$$

where r is the curve radius. Since both velocity and trajectory tracking must be realized, two reference signals given in reference vector R must be tracked: $R = [\dot{\xi}_{ref} \quad \dot{\psi}_{ref}]^T$.

The velocity error between the reference and the current velocity must be minimized with the optimization criterion:

$$z_{\xi} = |\dot{\xi}_{ref} - \dot{\xi}| \rightarrow min! \quad (6)$$

Moreover, the yaw rate error between the reference and the current yaw rate must be minimized as well with the optimization criterion:

$$z_{\dot{\psi}} = |\dot{\psi}_{ref} - \dot{\psi}| \rightarrow min! \quad (7)$$

Thus, a performance vector is defined as

$$z_1 = [z_{\xi} \quad z_{\dot{\psi}}]^T. \quad (8)$$

At the same time, the saturation of the actuators must be prevented. The maximum outputs of the in-wheel motors and the steering system are known by their physical construction limits and the road conditions. Considering these limits, a second performance vector is formulated as

$$z_2 = [F_l \quad \delta \quad M_z]^T. \quad (9)$$

The system matrix in (4) depends on the velocity of the vehicle $\dot{\xi}$ nonlinearly. By applying a scheduling variable

$$\rho_1 = \dot{\xi} \quad (10)$$

the nonlinear model is converted into an LPV model. In order to reconfigure the controller in case of adhesion loss in a wheel or a fault either in the in-wheel motors or in the operation of the steering, another scheduling variable ρ_2 is also introduced.

The controller is designed in such a way that in normal driving conditions the vehicle must be operated entirely with the torque generation of the in-wheel electric motors. It is assumed that owing to the accurate and fast response of the in-wheel motors it is possible to estimate the transmitted torque for each wheel. The estimation is based on the motion equation of the wheel, as follows:

$$J_\omega \dot{\omega} = T - R_{eff} F, \qquad (11)$$

where J_ω is the wheel inertia which is constant, $\dot{\omega}$ is the angular acceleration measured by the wheel sensor, R_{eff} is the effective rolling radius of the wheel, F is the drive force, T is the torque generated by the in-wheel motor. The drive force F and the corresponding transmitted torque can be estimated (for more details see [3]).

Hence, a ratio between the yaw moment M_z required by the high-level control and the transmitted yaw moment M_z^{trans} realized with the torque distribution between the four in-wheel engines can be defined. The transmitted yaw torque can be calculated as follows:

$$M_z^{trans} = \frac{-M_{fL}+M_{fR}}{R_{eff}} \frac{b_f}{2} + \frac{-M_{rL}+M_{rR}}{R_{eff}} \frac{b_r}{2} \qquad (12)$$

where b_f and b_r are the front and rear track width, and, moreover, M_{ij}, $i \in [f = front, r = rear]$, $j \in [L = left, R = right]$ are the transmitted torques of the front and rear wheels on the left and right. These torques are assumed to be estimated. Hence, the scheduling variable ρ_2 is defined as:

$$\rho_2 = \left| \frac{M_z - M_z^{trans}}{M_z} \right| \qquad (13)$$

The small value of ρ_2 shows that the desired yaw moment is realized acceptably, otherwise the difference between the desired and the current yaw moment must be reduced. If the difference is significant the vehicle is skidding with one of the wheels or a serious fault event in the in-wheel motor has occurred. The scheduling variable is scaled in order to provide the appropriate modification of the desired yaw moment. Note that in order to avoid the chattering of this scheduling variable ρ_2, a first-order proportional filter and a hysteresis component are applied. Thus, the performance degradation in the generation of the yaw moment is handled by the scheduling variable ρ_2.

The fault-tolerant control must handle the performance degradation or a fault of the steering. In this case the steering angle must be substituted for by additional yaw moment M_z^{add}, which is generated by in-wheel engine torques. This control problem can be solved if the steering fault has been detected and the control is designed by considering the detected fault. Based on the detected failure the scheduling variable ρ_3 is introduced in order to handle the steering angle. This variable is also scaled. A large value of ρ_3 guarantees that the high-level control does not require steering angle and the control task is solved by a greater yaw moment.

3 Reconfigurable control design

The control framework is based on a weighting strategy in a closed-loop interconnection structure, see Figure 2.

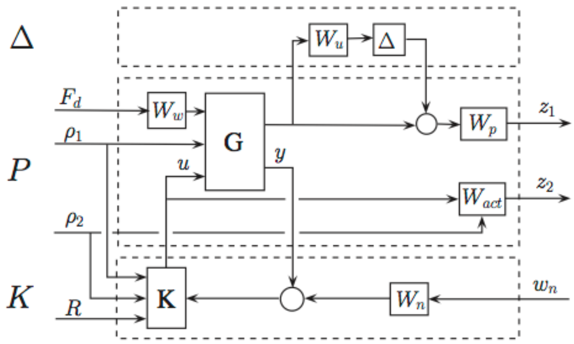

Figure 2: Closed-loop interconnection structure

The purpose of weighting function W_p is to ensure a trade-off between the performances. These weighting functions can be considered as penalty functions, thus weights should be large where small signals are desired and vice versa. Since the control goal is to track the road trajectory and the reference velocity at the same time, two performance weighting function is applied in a second-order proportional form: $W_p = (\alpha_2 s^2 + \alpha_1 s + 1)/(T_1 s^2 + T_2 s + 1)$, where $\alpha_{1,2}$ and $T_{1,2}$ are designed parameters. The purpose of the weighting functions W_w and W_n is to consider the disturbance and sensor noises, and are also chosen in a linear and proportional form. The uncertainties of the system (unmodelled dynamics, uncertain parameters) are handled by the Δ block, whereas the neglected dynamics is represented by the weighting function W_u.

The reconfiguration between the actuators, i.e. in-wheel motors and steering, is handled with the weighting function W_{act}. The purpose is to create the desired actuator selection, i.e applying steering intervention only if the desired yaw-moment is not feasible due to failure of an in-wheel engine or loss of adhesion. Thus, a weighting for the steering $W_{act\delta} = \rho_3/(\delta_{max}\beta_1)$ and for the yaw-moment $W_{actMz} = \rho_2/(M_{zmax}\beta_2)$ are also selected, where $\beta_{1,2}$ are designed parameters applied to the steering angle and the yaw moment, δ_{max} is the maximum steering angle, M_{zmax} is the maximum differential torque.

The LPV control approach is based on using parameter-dependent Lyapunov functions as suggested by [1],[12]. The quadratic LPV performance problem is to select the parameter-varying controller in a manner as to ensure the quadratic stability of the resulting closed-loop system and at the same time guarantee that the induced $\mathcal{L}_2$ norm from the disturbance to the performances is less than the value γ. The optimization task is the following:

$$\inf_K \sup_{\rho \in \mathcal{F}_\mathcal{P}} \sup_{\|w\|_2 \neq 0, w \in \mathcal{L}_2} \frac{\|z\|_2}{\|w\|_2} \leq \gamma. \qquad (14)$$

A Linear Matrix Inequalities (LMIs)-based solution is given for the quadratic LPV γ-performance problem, thus a feedback gain is computed for each vertex.

The reconfigurable control system is implemented in a hierarchical structure. The design of the multi-layer, reconfigurable control system can be seen in Figure 3.

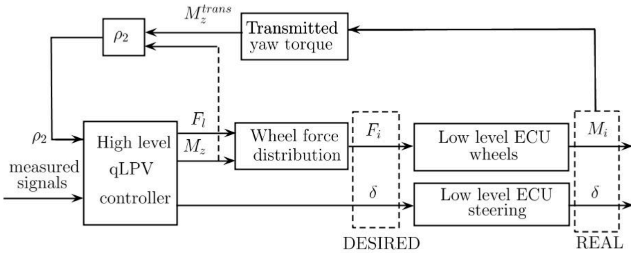

Figure 3: Architecture of control system

The purpose of the high-level controller in the first layer is to calculate the control inputs using the measured signals and the scheduling variable ρ_2. The purpose of wheel force distribution in the second layer is to distribute the longitudinal force and the yaw moment desired by the LPV control between the four in-wheel electric motors. In order to define the wheel torques, a dynamic allocation method is used combining details presented in [9],[15]. The pitch dynamics of the vehicle is considered assuming the longitudinal acceleration to be measured. Thus, the front and rear axle loads can be expressed as:

$$F_{zf} = \frac{mgl_2 - ma_x h}{(l_1+l_2)}, F_{zr} = \frac{mgl_1 + ma_x h}{(l_1+l_2)},$$

where h is the height of the center of gravity and a_x is the longitudinal acceleration. Accordingly, the load transfer distribution between the front and rear axles can be written as:

$$\frac{F_{zf}}{F_{zr}} = \frac{mgl_2 - ma_x h}{mgl_1 + ma_x h} = \kappa$$

The longitudinal force can be expressed by the axle load $F_i = \mu F_{zi}$, where μ is the longitudinal adhesion coefficient. In order to distribute the longitudinal load transfers, the coefficient κ is introduced: $F_f / F_r = \kappa$. Consequently, the following expressions are applied: $F_{rL} = \kappa F_{fL}$, $F_{rR} = \kappa F_{fR}$.

Assuming δ to be small, the longitudinal force F_l given by the high-level controller must satisfy the following equation:

$$F_l = F_{fL} + F_{fR} + F_{rL} + F_{rR}$$

where F_{ij} $i \in [f = front, r = rear]$, $j \in [L = left, R = right]$ are the longitudinal wheel forces of the front and rear wheels on the left and right. The required yaw moment M_z, which must be realized with the differential drive/brake torques of the in-wheel motors, is as follows:

$$M_z = (-F_{fL} + F_{fR})\frac{b_f}{2} + (-F_{rL} + F_{rR})\frac{b_r}{2} \qquad (15)$$

Consequently, the longitudinal force and the yaw moment are expressed as follows:

$$F_l = (F_{fL} + F_{fR})\left(1 + \frac{1}{\kappa}\right)$$
$$M_z = (-F_{fL} + F_{fR})\left(\frac{b_f}{2} + \frac{1}{\kappa}\frac{b_r}{2}\right)$$

Rearranging these equations the wheel forces are as:

$$F_{fL} = \frac{F_l}{2\left(1+\frac{1}{\kappa}\right)} - \frac{M_z}{b_f + \frac{1}{\kappa}b_r}, \quad F_{rL} = \frac{1}{\kappa}F_{fL},$$
$$F_{fR} = \frac{F_l}{2\left(1+\frac{1}{\kappa}\right)} + \frac{M_z}{b_f + \frac{1}{\kappa}b_r}, \quad F_{rR} = \frac{1}{\kappa}F_{fR}$$

Finally, the torques to be generated by the in-wheel motors can be expressed as $T_{ij} = R_{eff} F_{ij}$.

The third layer of the hierarchical control structure is responsible for tracking the allocated control forces by the low-level controllers, i.e the steering system and the in-wheel motors. Hence, these controllers transform the steering angle and the in-wheel motor torques into real physical parameters of the actuator.

The low-level current control of the in-wheel motors is not studied in this paper, but it has been investigated by several authors, see [13],[14]. Instead, a simplified model is applied in order to relate the torque command defined by the first two layers of the hierarchical control structure and the motor torque generated by the electric motor. For this purpose, a first-order transfer function is used as follows:

$$T_{motor}(s) = \frac{1}{1 + (L_m/R_m)s} T$$

where T_{motor} is the generated in-wheel electric motor torque, T is the desired torque given by the dynamic allocation method listed above, L_m and R_m are the motor inductance and resistance, respectively.

4 Simulation results

The simulation vehicle is driven by four in-wheel motors and a steering system. In the simulation example the in-wheel vehicle must perform trajectory tracking, which is defined by its reference yaw rate and velocity, see Figure 4.

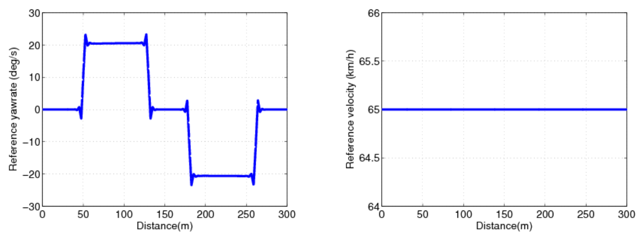

(a) Reference yaw rate (b) Reference velocity

Figure 4: Reference signals

The analysis of the designed controller is performed by using the CarSim software. In this software the model of the vehicle dynamics is represented with high accuracy.

The first simulation example presents the operation of the in-wheel electric vehicle. The reference yaw rate and velocity are generated by both in-wheel electric motors and steering. The designed high-level control signals, i.e., the longitudinal forces, the yaw moment and the steering angle, are presented in Figure 5(a)...5(c), while the implemented low-level control signals, i.e., the in-wheel electric motor torques are in Figure 5(d). The steering angle is in the ±2.5deg interval, the longitudinal forces are below 550N, the yaw moment is in the ±1000Nm interval, while the electric motor torques are between -100Nm and +200Nm. During maneuvers the vehicle slips increase both in the longitudinal and the lateral directions. The longitudinal wheel slips are below 0.02 and lateral side-slip angles are below 2.5deg, which are illustrated in Figures 5(e) and 5(g), respectively. The performance signals, i.e., the yaw-rate error and the velocity error, are shown in Figures 5(f) and 5(h), respectively. The lateral deviation from the centerline of the road during the maneuver is within 0.3m, which is also acceptable.

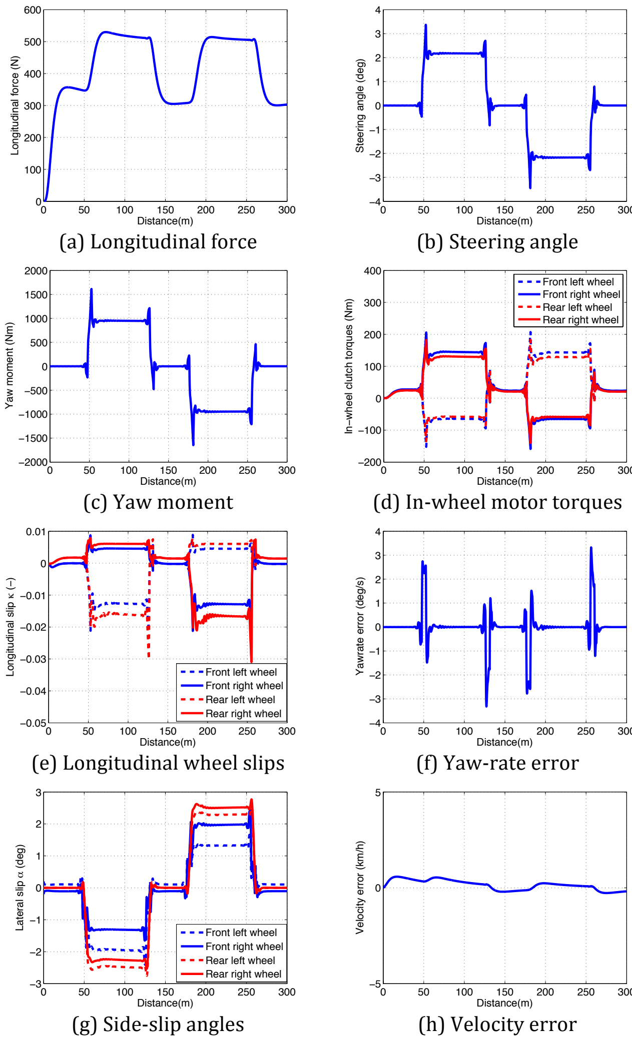

(a) Longitudinal force (b) Steering angle

(c) Yaw moment (d) In-wheel motor torques

(e) Longitudinal wheel slips (f) Yaw-rate error

(g) Side-slip angles (h) Velocity error

Figure 5: Time responses of the in-wheel electric vehicle

The second simulation demonstrates the effectiveness of the proposed reconfigurable control when an in-wheel motor failure has occurred. It is assumed that the front electric motor at the left-hand-side has broken down, so that the electric motors themselves are not able generate the required yaw moment. Consequently, in the left bends the lateral error increases and the performance of the control system is degraded. In the reconfigurable control the insufficient yaw moment is compensated for by the steering system. The steering angle is increased in order to guarantee the required lateral displacement. The high-level control signals are illustrated in Figure 6(a)...6(c), while the low-level wheel motor torques are in Figure 6(d). The steering angle increases to the ±3deg interval, the longitudinal forces tend to 1500N, the yaw moment is between -500Nm and 800Nm. The electric motor torques are usually within the -100Nm and +200Nm interval, however, the rear motor on the left is increased to 250 Nm. During maneuvers the longitudinal wheel slips are increased to 0.03, see Figures 6(f). Although both the yaw-rate error (see Figures 6(e)) and the velocity error increase, they remain within acceptable limits.

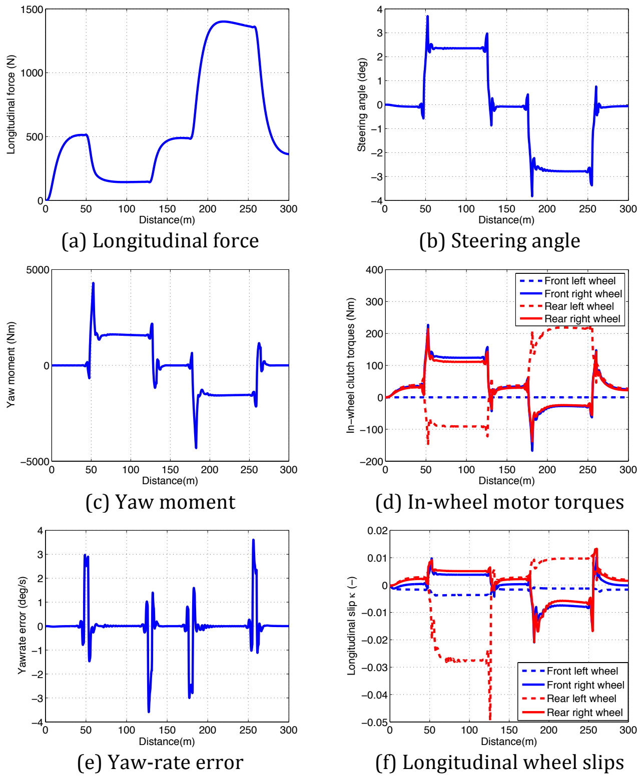

(a) Longitudinal force (b) Steering angle

(c) Yaw moment (d) In-wheel motor torques

(e) Yaw-rate error (f) Longitudinal wheel slips

Figure 6: Time responses of the vehicle when an in- wheel motor failure has occurred

In the third example, a fatal error has occurred in the operation of the steering system, thus the vehicle operates only with the four in-wheel motors. The in-wheel motors generate the required yaw moment for trajectory tracking in such a way that the steering angle is substituted for. The high-level control signals are illustrated in Figures 7(a)...7(c), while the low-level wheel clutch torques are in Figure 7(d). The longitudinal forces tend to 600N, the yaw moment is in the ±1000Nm interval, while the electric motor torques are in the ±200Nm interval. During maneuvers the vehicle slips significantly increase both in the longitudinal and lateral directions. The longitudinal wheel slips are between –0.07 and 0.02 and the lateral side-slip angles increase signficantly to 4deg, which are illustrated in Figures 7(e) and 7(f), respectively. Although both the yaw-rate error (see Figures 6(e)) and the velocity error increase, they remain within acceptable limits.

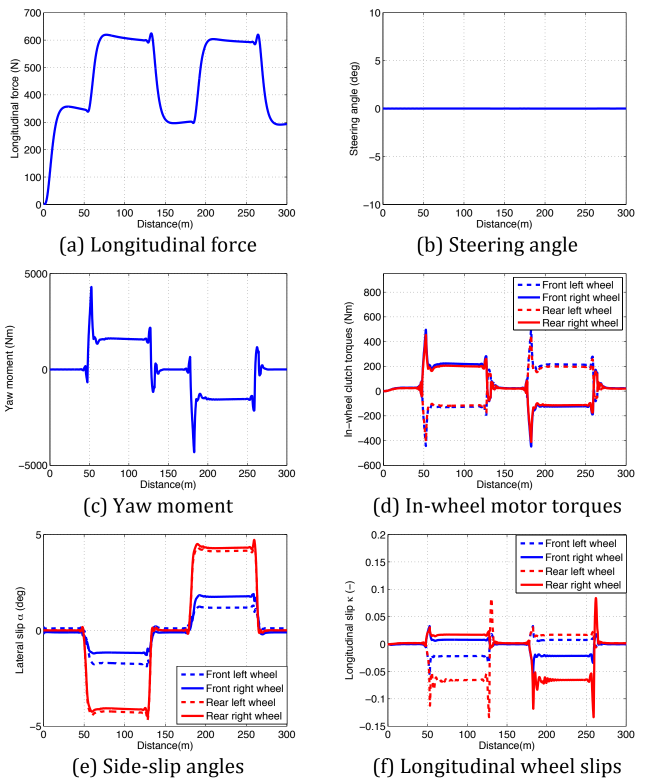

(a) Longitudinal force (b) Steering angle

(c) Yaw moment (d) In-wheel motor torques

(e) Side-slip angles (f) Longitudinal wheel slips

Figure 7: Time responses of the vehicle when a fatal error has occurred in the steering system

5 Conclusion

The paper has proposed a reconfiguration control method for an electric vehicle operated by four in-wheel hub motors and a steering system. The direction of the vehicle is based on the steering, while driving and braking are based on the electric motors. The reconfigurable control is activated when skids or a failure have occurred. The control design is based on the LPV method, in which performance specifications and fault scenarios are built in by scheduling variables. The designed high-level control signals are transformed into electric motor torques, which are realized in the low level. The reconfigurable control system is implemented in a hierarchical structure.

References

[1] J. Bokor and G. Balas. Linear parameter varying systems: A geometric theory and applications. *16th IFAC World Congress, Prague*, 2005.

[2] R. Castro, R. E. Araújo, M. Tanelli, S. M. Savaresi, and D. Freitas. Torque blending and wheel slip control in evs with in-wheel motors. *Vehicle System Dynamics*, 50:71–94, 2012.

[3] J.-S. Hu and D. Yin. Mtte-based motion stabilization control for in-wheel motor electric vehicles. *SICE Annual Conference September 13-18, 2011, Tokyo, Japan*, 2011.

[4] J.-S. Hu, D. Yin, and Y. Hori. Fault-tolerant traction control of electric vehicles. *Control Engineering Practice*, pages 204–213, 2011.

[5] C.J. Ifedi, B.C. Mecrow, S.T.M. Brockway, G.S. Boast, G.J. Atkinson, and D. Kostic-Perovic. Fault tolerant in-wheel motor topologies for high performance electric vehicles. *IEEE Trans. on Industry Applications*, 49:1249 – 1257, 2013.

[6] K. Kawashima, T. Uchida, and Y. Hori. Rolling stability control based on electronic stability program for in-wheel-motor electric vehicle. *World Electric Vehicle Journal*, 3:1–8, 2009.

[7] M. Ringdorfer and M. Horn. Development of a wheel slip actuator controller for electric vehicles using energy recuperation and hydraulic brake control. *IEEE International Conference on Control Applications, Denver, USA*, pages 313–318, 2011.

[8] Y. Shibahata, K. Shimada, and T. Tomari. Improvement of vehicle maneuverability by direct yaw moment control. *Vehicle System Dynamics*, 1993.

[9] Z. Shuai, H. Zhang, J. Wang, J. Li, and M. Ouyang. Lateral motion control for four-wheel-independent-drive electric vehicles using optimal torque allocation and dynamic message priority scheduling. *Control Engineering Practice*, 24:55–66, 2013.

[10] B. Wang, X. Huang, J. Wang, X. Guo, and X. Zhu. A robust wheel slip ratio control design combining hydraulic and regenerative braking systems for in-wheel-motors-driven electric vehicles. *Journal of the Franklin Institute*, 50:71–94, 2014.

[11] R. Wang and J. Wang. Fault-tolerant control for electric ground vehicles with independently-actuated in-wheel motors. *Journal of Dynamic Systems, Measurement, and Control*, 134, 2012.

[12] F. Wu, X. H. Yang, A. Packard, and G. Becker. Induced l^2-norm control for LPV systems with bounded parameter variation rates. *International Journal of Nonlinear and Robust Control*, 6:983–998, 1996.

[13] F.-K. Wu, T.-J. Yeh, and C.-F. Huang. Motor control and torque coordination of an electric vehicle actuated by two in-wheel motors. *Mechatronics*, 23:46–60, 2013.

[14] Y.-P. Yang and C.-P. Lo. Current distribution control of dual directly driven wheel motors for electric vehicles. *Control Engineering Practice*, 16:1285– 1292, 2008.

[15] H. Zhao, B. Gao, B. Ren, and H. Chena. Integrated control of in-wheel motor electric vehicles using a triple-step nonlinear method. *Journal of the Franklin Institute, Article In Press*, 2014.